NASA TECHNICAL NOTE

NASA TN D-4552
c. 1

NASA TN D-4552

THE INTERPRETATION OF DAYTIME MEASUREMENTS BY THE NIMBUS I AND II HIGH RESOLUTION INFRARED RADIOMETERS

by G. Kuers

Goddard Space Flight Center
Greenbelt, Md.

THE INTERPRETATION OF DAYTIME MEASUREMENTS BY THE NIMBUS I AND II

HIGH RESOLUTION INFRARED RADIOMETERS

By G. Kuers

Goddard Space Flight Center
Greenbelt, Md.

NATIONAL AERONAUTICS AND SPACE ADMINISTRATION

ABSTRACT

Dense cumulus clouds and fog banks have been selected to determine mean values of their reflectances by means of the High Resolution Infrared Radiometers (HRIR) of Nimbus I and Nimbus II in the wavelength region between 3.6μ and 4.2μ. While both instruments yielded satisfactory results at night, it became apparent that Nimbus I delivered too high reflectance values by day. It was concluded that spurious shortwave radiation entered the radiometer. The amount of the energy difference was used to determine the most probable cause of the malfunctioning, which was considered to be an uncoated rim or a crack of the interference filter.

CONTENTS

THE INTERPRETATION OF DAYTIME MEASUREMENTS BY THE NIMBUS I AND II HIGH RESOLUTION INFRARED RADIOMETERS

by
G. Kuers*
Goddard Space Flight Center

INTRODUCTION

One of the Nimbus satellite experiments concerns cloud mapping by the High Resolution Infrared Radiometer (HRIR), (References 1 to 3). Its spectral region, between 3.6μ and 4.2μ, was originally intended to obtain maps of clouds and the earth during the night, by means of the emitted thermal radiation. During daytime, observations with limited accuracy are possible, but the intensities have to be interpreted as reflected solar radiation superimposed on emitted thermal radiation.

Despite the uncertainties of the daytime measurements caused by the thermal radiation of the clouds, a discrepancy between the results of HRIR I and HRIR II became apparent. It is the intention of this investigation to discover to what degree the daytime results differ, to consider the various possible sources of error, and — since we have no access to the orbiting spacecraft — to determine the most probable cause of the malfunctioning.

SOME PROPERTIES OF CLOUDS TO BE CONSIDERED FOR CLOUD
REFLECTANCE COMPARISONS

Since the reflection of solar radiation by clouds is caused by scattering by the cloud droplets (according to Mie's theory), the scattered radiation can be expected to be highly anisotropic and therefore dependent on the scattering angle, the droplet size distribution, and the water content and thickness of the cloud (Reference 4). The thermal emission of the cloud surface has a considerable influence on reflectance measurements in the spectral region of the HRIR. The measurement can be affected also by the cloud size, if it does not completely fill the radiometer's field of view.

Since we have no immediate information about the physical properties of the observed clouds, we are forced to choose for comparison those clouds that seem to have nearly identical radiation features. Extended stratocumuli or fog banks seem to be fairly well suited for this purpose. These types of cloud substantially fulfill the requirements of large clouds and can be recognized as dense water clouds. They should be completely opaque and not exhibit any noticeable structure. This property can best be proved if the background is an ocean surface, because the latter shows nearly no structure in its radiation features.

Stratocumuli and fog have fairly high reflectances and are, therefore, also well suited for determining any difference between the reflectance values obtained from Nimbus I and those from Nimbus II. However, these cloud types have low altitudes and associated high temperatures, which result in much thermal radiation leaving the cloud surface and affecting the reflection measurements. This effect causes an uncertainty in calculating reflectance. Also, some doubts remain whether the observed cloud retained its temperature and structure between daytime and nighttime measurements. This is especially true for fog that can disappear within a few hours — not to speak of its structure changes.

INVESTIGATION OF SOME CLOUDS

HRIR data of both satellites have been selected, using photofacsimile strips that permit a quick survey of the infrared pattern for each orbit. Advantage was taken of the Advanced Vidicon Camera System (AVCS), which provides additional visible pictures of the clouds to ensure that the area under observation is indeed a cloud and not perhaps a ground surface with similar emitting and reflecting properties.

Sun and observation zenith angles must be determined in each case, but only those cases will be selected where both angles are sufficiently small. Then the observation covers backscattering within a small range of scattering angle.

Investigations of selected clouds have been performed using Mercator Grid Print Maps in 1:1,000,000 scale which contain intensity values in terms of effective temperatures. The choice of the scale has some influence on the readings, because extreme values would be smoothed by a coarser scale.

The effective temperature T_{BB} is related to the effective radiance $\bar{N}$, within the spectral region of the radiometer, by

$$\bar{N} = \int_{\lambda_1}^{\lambda_2} \phi_\lambda \, B_\lambda \left(T_{BB}\right) d\lambda \quad , \tag{1}$$

where $B_\lambda(T_{BB})$ is the radiance of a blackbody of temperature T_{BB}, and ϕ_λ is the spectral responsivity of the radiometer. During daytime, the effective radiance is

$$\overline{N}_D = \int_{\lambda_1}^{\lambda_2} \phi_\lambda \left[(1-R)B_\lambda(T_{BB}) + RH \cos z/\pi\right] d\lambda \quad , \tag{2}$$

where R is the reflectance of the surface under observation. Its wavelength dependency, although present for clouds, can be neglected for comparison purposes. Equation 2 contains the simplifying assumption of isotropically reflecting clouds; therefore, their radiance is $RH \cos z/\pi$, where $H \cos z$ is the irradiance of the cloud and z is the zenith angle of the sun. Neglecting anisotropy does not affect the following evaluations, since only cases of scattering angles within a sufficiently small range will be considered.

Equation 2 has been used for plotting a set of curves for which $r = R \cos z$. R itself can readily be obtained if the surface temperature of the cloud is taken into account. Since Nimbus II uses an improved interference filter with higher transmittance as well as with higher responsivity at shorter wavelengths (Figure 1), Equation 2 was used separately for each radiometer (Figures 2 and 3). Higher short-wavelength responsivity causes increased effective temperatures for a given reflectance.
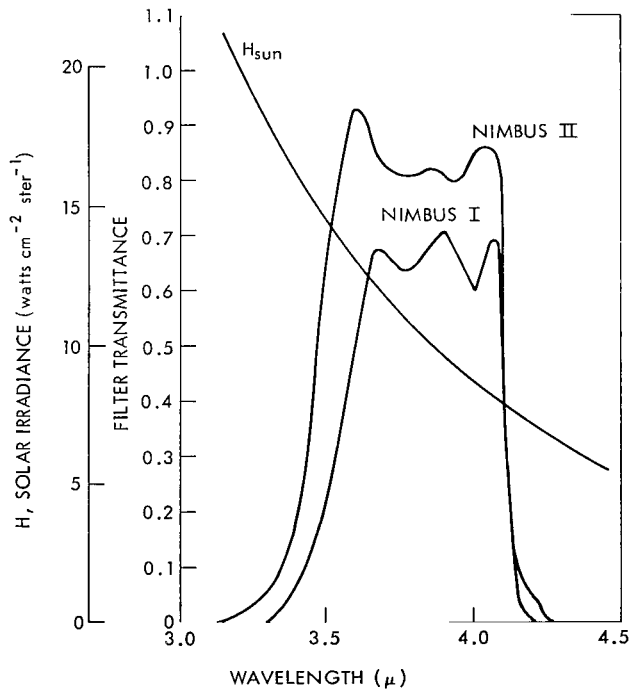
In order to obtain representative values of cloud reflectances from grid print maps, frequency distributions of the effective cloud

Figure 1—Solar irradiance and filter transmittances of HRIR I and HRIR II.
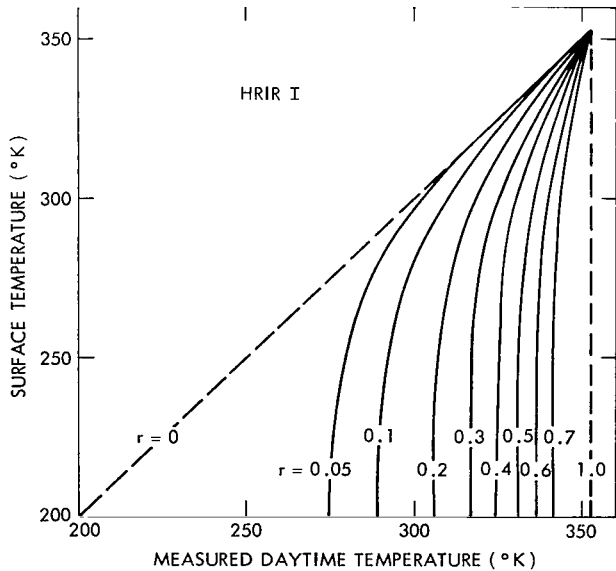

Figure 2—Relation between reflectance, surface temperature, and daytime temperature, HRIR I.

3
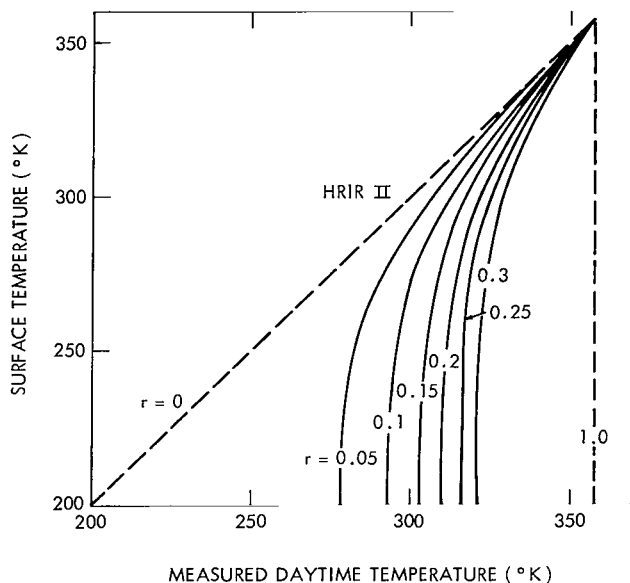
Figure 3—Relation between reflectance, surface temperature, and daytime temperature, HRIR II.

temperatures associated with the distribution maxima are considered representative. Besides this, shapes of the frequency distributions yield some information about cloud structures, as we shall see.*

Unfortunately, with perhaps one exception, it was impossible to determine the daytime surface temperature of the clouds by nighttime measurements, 12 hours earlier or later. Observations made 12 hours apart generally showed that the homogeneous, widespread cloud surface observed in the daytime was broken, scattered, or even nonexistent. There exists in principle the possibility of determining the surface temperature by simultaneous measurements of the Medium Resolution Radiometer (MRIR) in the 10- to 11-micron channel. However, since this possibility applies only to Nimbus II and we are primarily interested in resolving the discrepancy between both cloud reflectance measurements, we may forego a precise determination of the surface temperature. Moreover, we know that its influence is small compared to the relatively high reflected intensity of the clouds. Thus, as a first-order approximation, we assume an equal cloud height in every case and estimate the temperature of the cloud by applying an equal temperature gradient to the appropriate sea temperature.

The first case chosen was a cloud observed by Nimbus I over an area about 8 degrees west of the shore of Chile. The enlarged photofacsimile and the AVCS picture are shown in Figures 4 and 5. From the frequency distribution in Figure 6, an effective cloud temperature of 317.5°K can be read off. The steep slopes of the distribution confirm that the cloud has indeed highly uniform radiation features. (The white rhombus superimposed on Figure 4, and similarly geometric figures on other photos, demarcate the area from which data shown in graphs were obtained.)

Another case chosen was likewise observed by Nimbus I over an area in the South Pacific (Figures 7 and 8). In Figure 9, four frequency distributions are plotted. Three of them refer to three selected narrow strips shown in Figures 7 and 8, north-south oriented, according to the specifications in Figure 9, and intentionally including areas with broken clouds in the north and the south. The fourth curve refers to one of these three regions but does not include the broken clouds at the edge of the cloud.

---

*The frequency distribution allows us also to determine the degree of uncertainty of temperature measurements due to noise fluctuations, if the radiation field is sufficiently uniform.
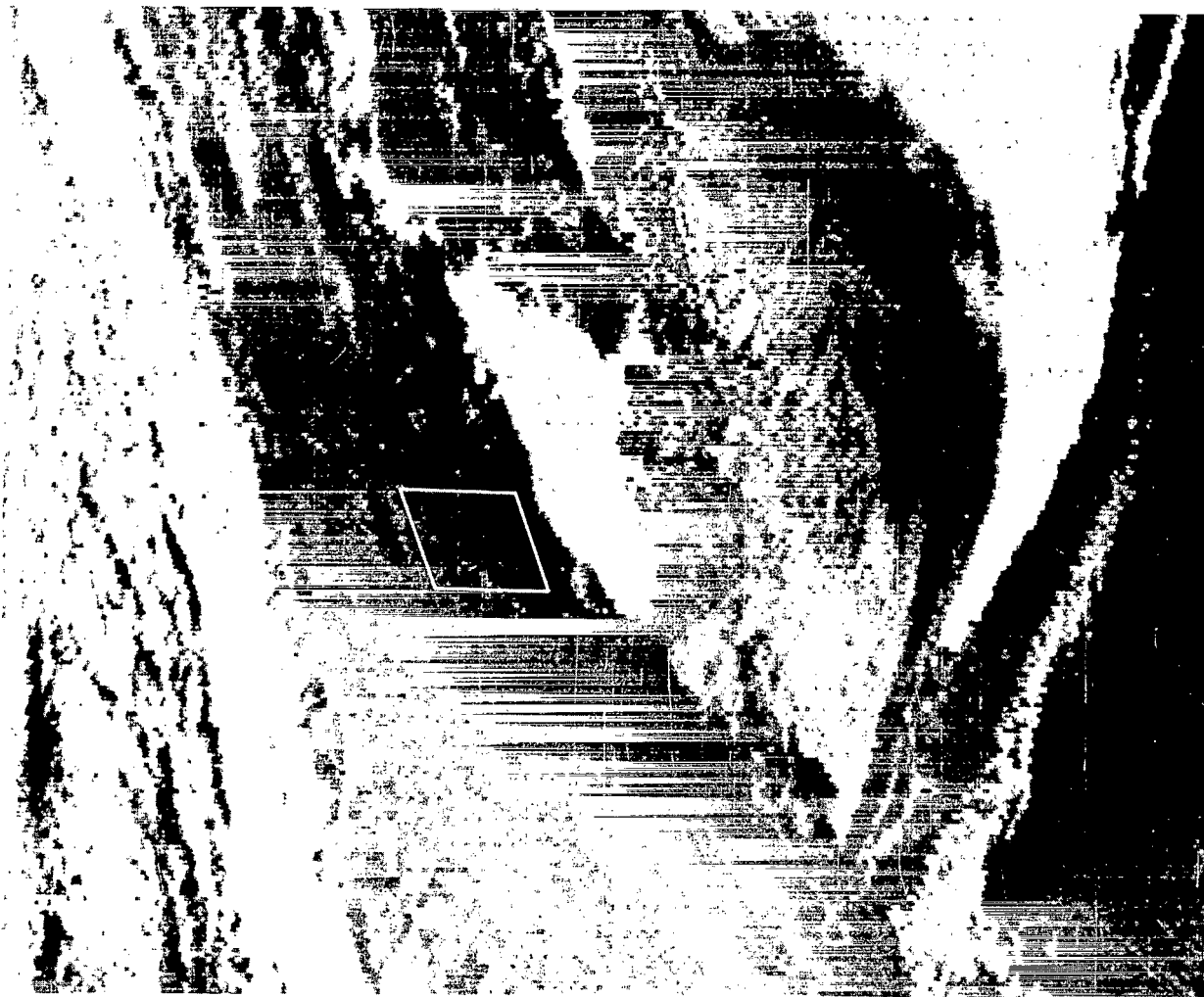
Figure 4—Photofacsimile, HRIR I, Sept. 11, 1964, Orbit 210, 36.5°S, 84°W.

A comparison of one of the broken cloud distributions with that for the smooth cloud part makes it clear that the temperature corresponding to the maximum of the frequency distribution really represents the mean value of the effective temperature, because its position is obviously not affected by broken parts of the cloud. These parts seem only to decrease the steepness of the low-temperature slope, causing the distribution curve to fall off to the effective temperature of the ocean. We recognize further that the position of the maximum is the same within a longitude range of 9.5 degrees, a fact which confirms that the cloud is really highly homogeneous with an effective temperature of 315°K.

Fortunately, it was possible to retrace the cloud system to a nighttime orbit, seven orbits before (Figure 10 shows the photofacsimile and Figure 11 the frequency distribution). From the

5

Figure 5—AVCS picture, Sept. 11, 1964, Orbit 210, 36.5°S, 84°W.
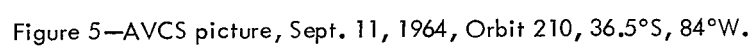
photofacsimile, three intensity ranges can be clearly discerned. In the south a low-emitting region is present — apparently high clouds. The central part of the reprint is gray-shadowed, showing our cloud system in a southwesterly direction from the point where it appeared about 12 hours later. The gray tone and the fairly high homogeneity of the cloudy area confirm that the cloud is one of the low-altitude, high-emitting type. Only some portions in the north show still higher temperature. Most likely they are spots of open sea unobscured by broken clouds. The mean temperature of the cloud can be determined from the frequency distribution as 278°K.

A third cloud system was selected not very far south from the second case discussed (see Figures 12 and 13). The frequency distribution in Figure 13 shows that apparently the observed cloud part is also smooth, since the maximum, which occurs at about 314°K, is fairly well pronounced.

Figure 6—Frequency distribution of daytime temperature, HRIR I, Sept. 11, 1964, Orbit 210, 36.5°S, 84°W.

A nighttime observation (Figure 14)*, again about 12 hours earlier, produced a cloud surface temperature measurement of about 280°K, obtained from the frequency distribution in Figure 15. A remarkable feature of the distribution is that when the temperature is decreased the frequency falls off sharply at about 280°; when the temperature is increased, the frequency falls off more slowly. This situation is caused by broken clouds which partially obscure the ocean, thus causing the slow fall-off to high temperatures; while the sharp cutoff indicates, most probably, the surface temperature of the cloud.

The first case chosen from Nimbus II was a fog bank west of Spain (Figures 16 and 17). The maximum of the frequency distribution in Figure 18 shows an effective cloud temperature of about 306°K. The slopes are fairly steep; however, the curve seems to be broader than the corresponding curves from Nimbus I.[†]

As a second case, an extended cloud south of the French Riviera was selected (Figures 19 and 20). From the AVCS picture, it can be recognized that South Europe, the Mediterranean Sea, and North Africa are covered with dense haze. Less pronounced, but still recognizable, is the haze layer in the photofacsimile, where it occurs as dark spots, especially over Spain and a large one
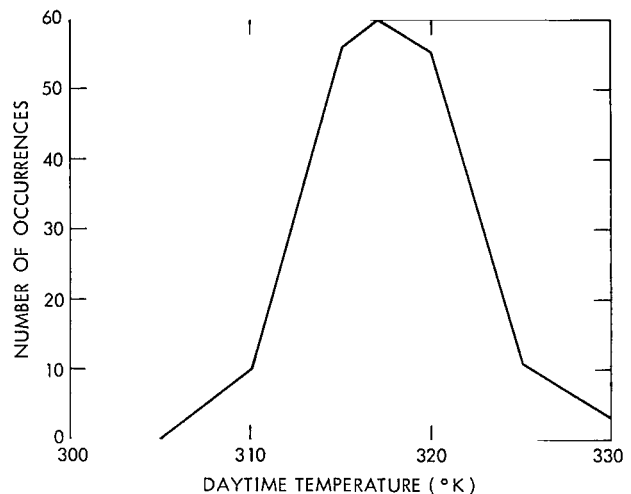
---

*The size of the smallest of the gray spots approaches the resolution of the instrument, thus simulating a fairly uniform cloud size distribution which is probably not present in reality.

[†]It appears that the other cases of Nimbus II also show somewhat broader distributions. This can be expected, since the effective radiance is always smaller, thus causing a decreased signal-to-noise ratio.
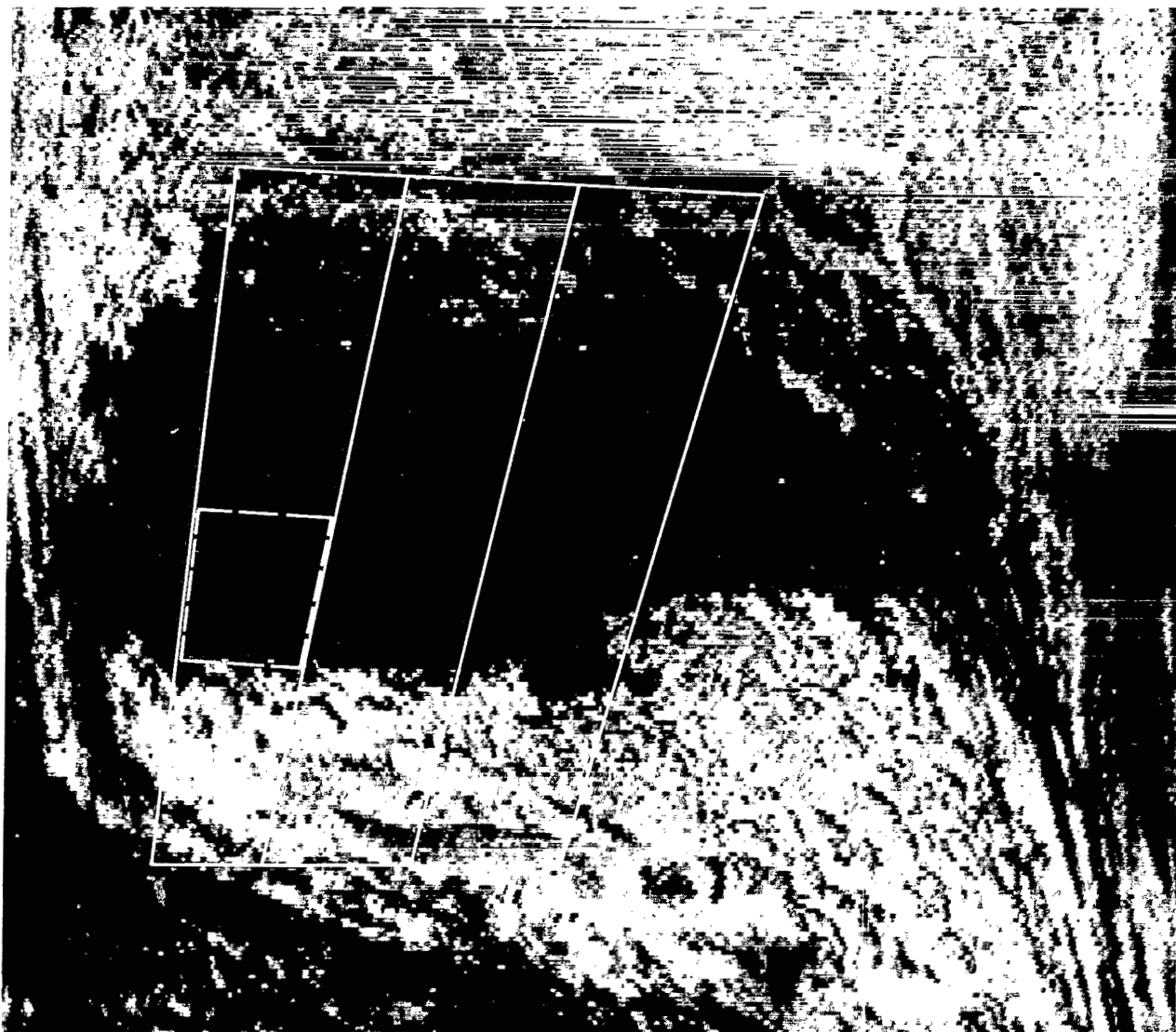
Figure 7—Photofacsimile, HRIR I, Sept. 2, 1964, Orbit 80, 27°S, 126°W.

over the Mediterranean Sea and the coast of Africa. It is, therefore, to be expected that the frequency distribution will not be as smooth as in the foregoing cases. Indeed, as Figure 21 shows, it even possesses three maxima. That they are real has been proved by counting slightly different areas several times. A possible explanation is given by the assumption that the maxima are related to three different reflecting layers, namely, the ocean, the cloud, and the haze layer, with the last two being not quite opaque, or at least having transparent areas. Since it is not quite clear how the maxima came about, the maximum at 305°K will be taken for the present
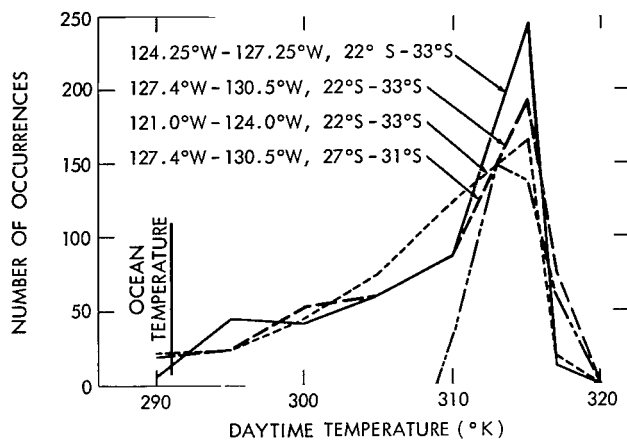
Figure 8—AVCS picture, HRIR I, Sept. 2, 1964, Orbit 80, 27°S, 126°W.

Figure 9—Frequency distribution of daytime temperature, HRIR I, Sept. 2, 1964, Orbit 80, 27°S, 126°W.
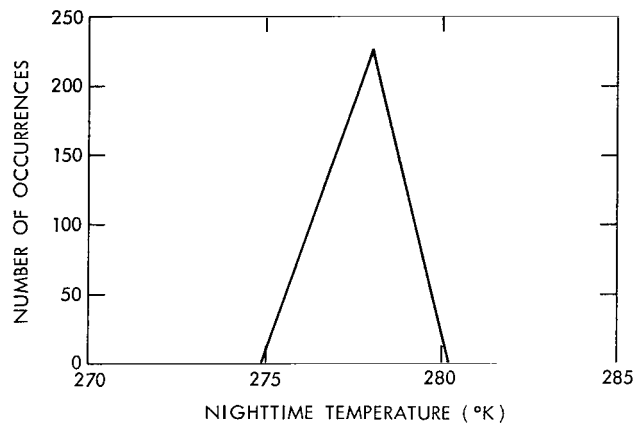

Figure 11—Frequency distribution of nighttime temperature, HRIR 1, Sept. 2, 1964, Orbit 73, 29.5°S, 132°W.
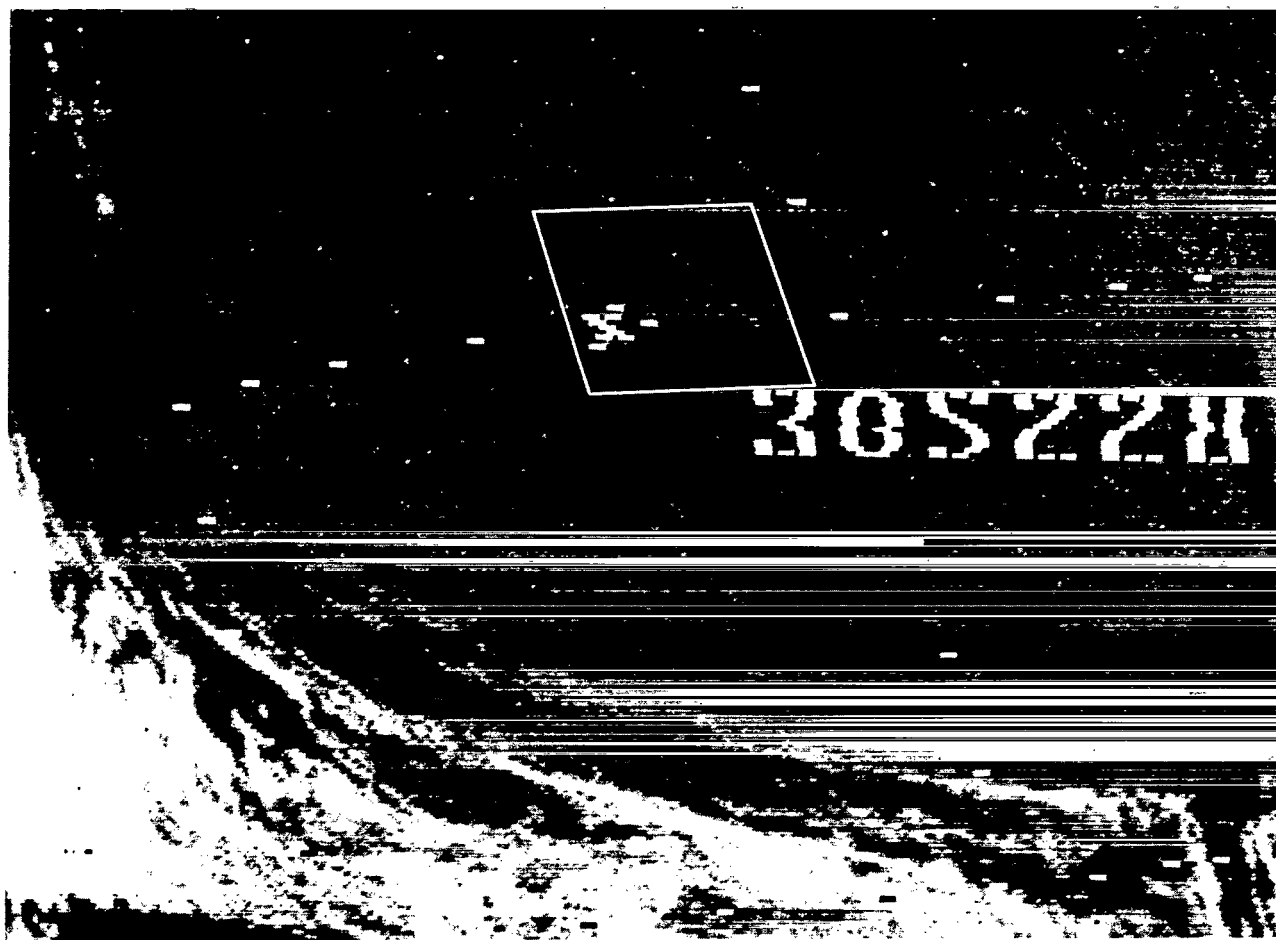

Figure 10—Photofacsimile, HRIR I, Sept. 2, 1964, Orbit 73, 29.5°S, 132°W.
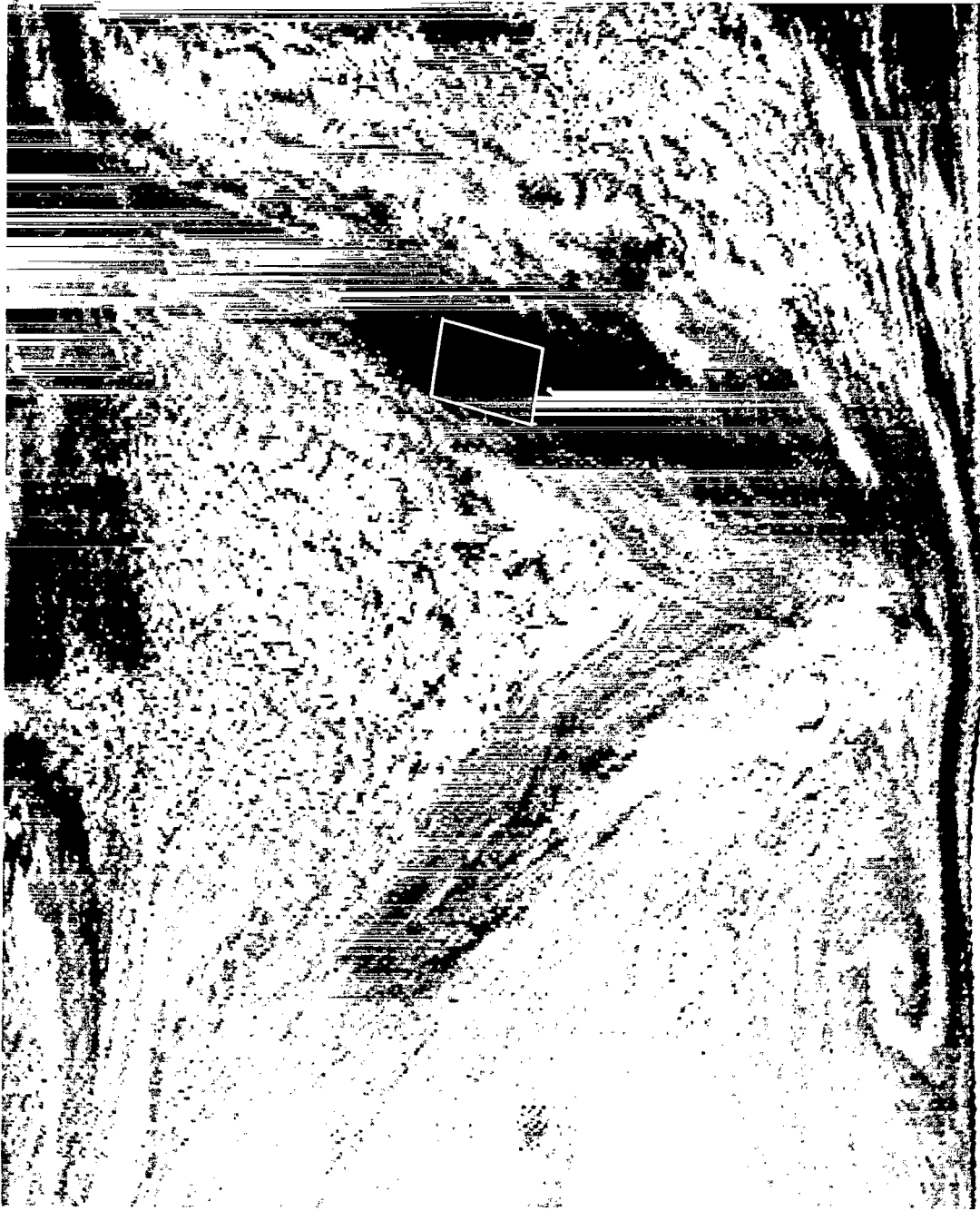
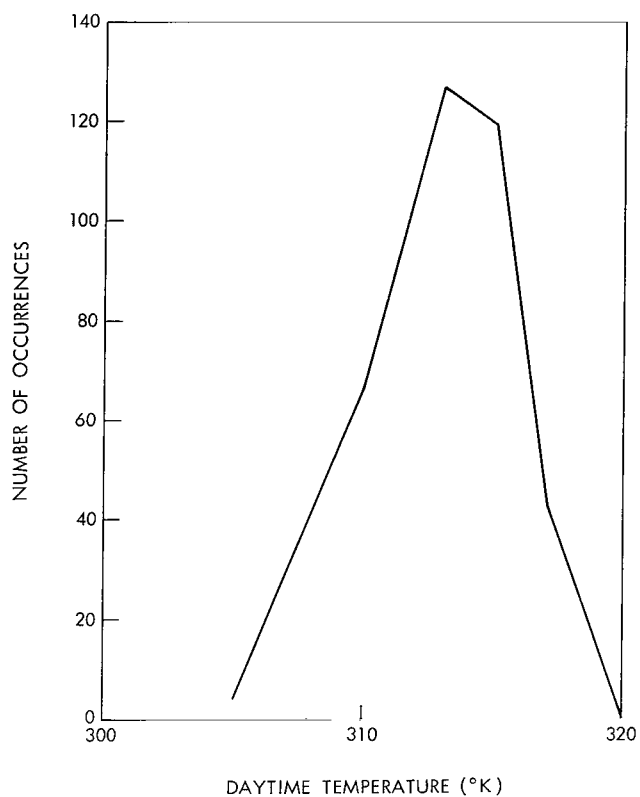Figure 12—Photofacsimile, HRIR I, Sept. 2, 1964, Orbit 80, 38°S, 116.5°W.

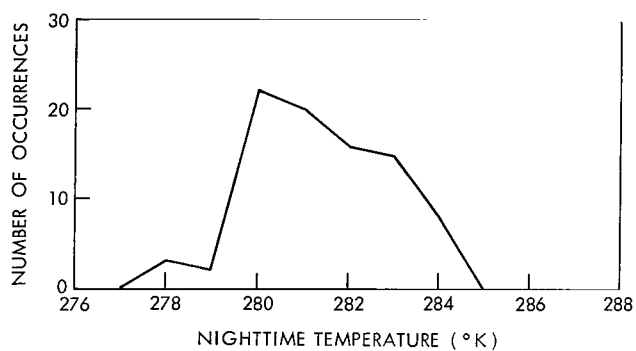Figure 13—Frequency distribution of daytime temperature, HRIR, Sept. 2, 1964, Orbit 80, 38°S, 116.5°W.

Figure 15—Frequency distribution of nighttime temperature, HRIR I, Sept. 2, 1964, Orbit 73, 47°S, 139°W.

as a representative value of the effective temperature.

A third case was selected from the same Nimbus II orbit as the second, but west of Spain. A cloud occurs there, separated from the land only by a small strip of open sea. (see Figure 16). The effective temperature can be determined as 305°K (Figure 22).
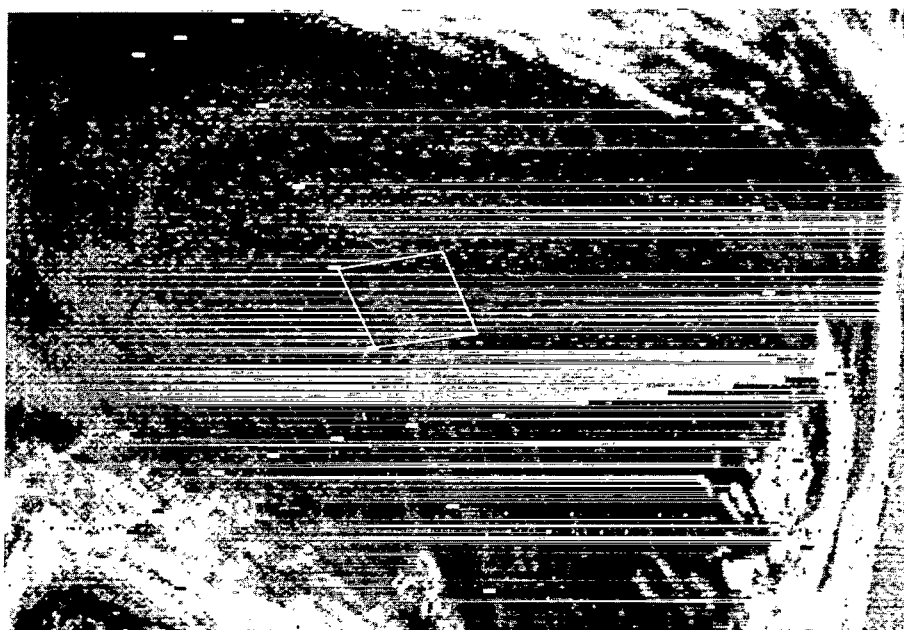

Figure 14—Photofacsimile, HRIR I, Sept. 2, 1964, Orbit 73, 47°S, 139°W.

COMPARISON OF DAYTIME RESULTS
OF BOTH RADIOMETERS

Cloud reflectances have been evaluated, assuming an equal cloud height of 2,000 meters and a vertical temperature gradient of 6°/km, and taking into account the monthly mean value of the ocean temperature (Reference 5).

Reflectance. values obtained from Nimbus I range between 22.8 percent and 32.4 percent. The mean value of the reflectance is 26.6 percent, and the appropriate effective radiance is 3.2×10^{-5} watts^{-2} cm^{-2} ster^{-1}. For Nimbus II, the cloud reflectance values range between 12.5 and 13.6 percent. The mean value is 12.9 percent, and the effective radiance is 2.7×10^{-5} watts^{-2} ster^{-1}. The radiance difference that must now be discussed is 5×10^{-6} watts-cm^{-2} ster^{-1}.

The discrepancy exists only during daytime. Allison and Kennedy (Reference 6) have compared nighttime measurements over oceans, performed by Nimbus I, with those made from ships and airplanes, and they found satisfactory agreement. Warnecke et al. (Reference 7) have investigated Nimbus II HRIR measurements over oceans through clear skies during the nighttime and also have found good agreement with simultaneous measurements of the surface temperature made from airplanes and ships. Thus the discrepancy seems to depend on the presence of the intensive solar short-wavelength radiation. This finding means that the wavelength responsivity of one (or both) of the radiometers is different from that assumed. Since the lead selenide detector is used at its responsivity peak and since an interference

Figure 16—Photofacsimile, HRIR II, May 21, 1966, Orbit 82, 42°N, 10°W.
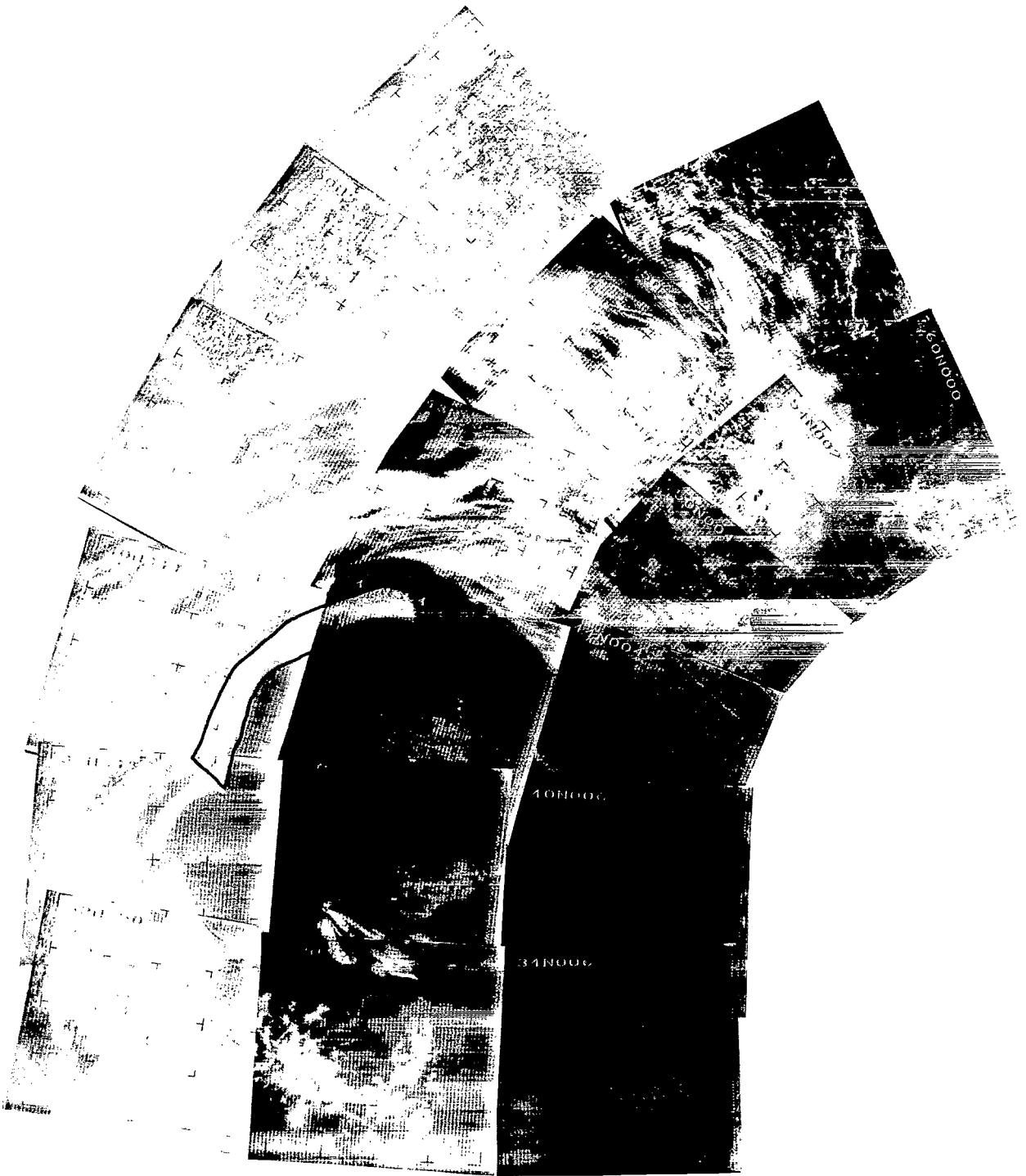
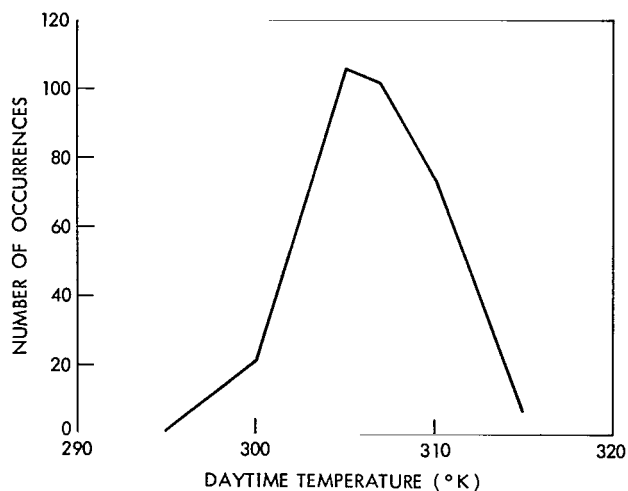Figure 17—AVCS picture, HRIR II, May 21, 1966, Orbit 82, 42°N, 10°W.

Figure 18—Frequency distribution of daytime temperature, HRIR II, May 21, 1966, Orbit 82, 42°N, 10°W.

filter with a relatively small bandwidth is employed, a change of the spectral transmittance of the filter is much more probable than a change of detector sensitivity.

Another question that arises in this connection is: which of the HRIR's may have delivered erroneous results? Comparisons of the HRIR data with cloud reflectance values obtained by Blau et al. (Reference 8) seem to indicate that cloud reflectances are well below the values obtained by Nimbus I (Figure 23). Although conclusions of greater precision cannot be drawn from Blau's results because his investigations do not go beyond 3.6μ, it will be assumed that the erroneous values are those of Nimbus I.

Figure 19—Photofacsimile, HRIR II, May 22, 1966, Orbit 95, 41.5°N, 4.5°E.

The following possible sources of error now seem worthy of investigation:

1. Assumption of additional transmission peaks of the filter at short wavelengths.

2. Assumption of a filter shift towards shorter wavelengths.

3. Assumption of additional unfiltered radiation reaching the detector.
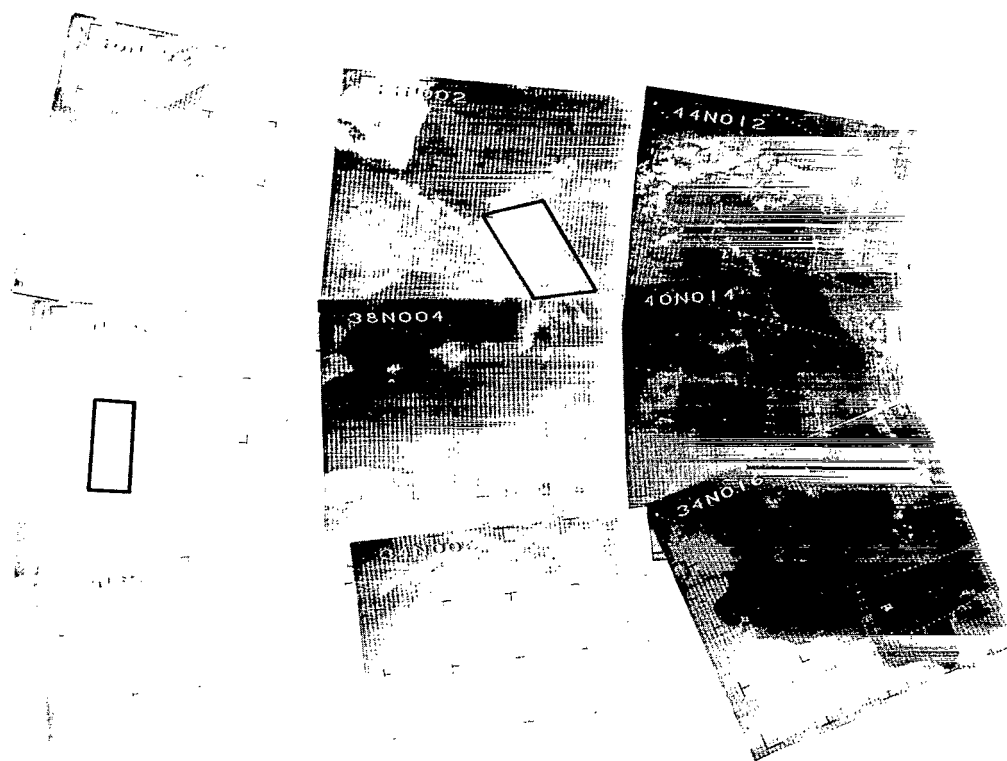
15

Figure 20—AVCS picture, HRIR II, May 22, 1966, Orbit 95, 41.5°N, 4.5°E.
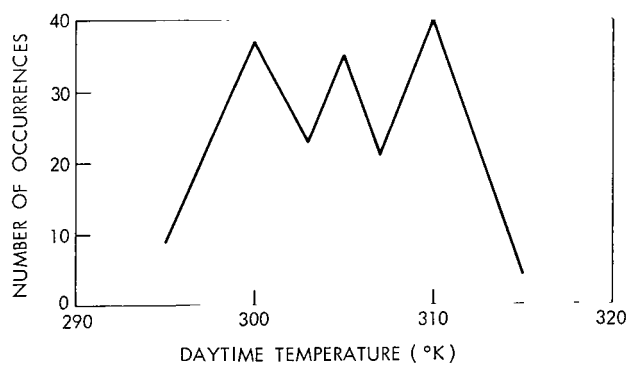

Figure 21—Frequency distribution of daytime temperature, HRIR II, May 22, 1966, Orbit 95, 41.5°N, 4.5°E.
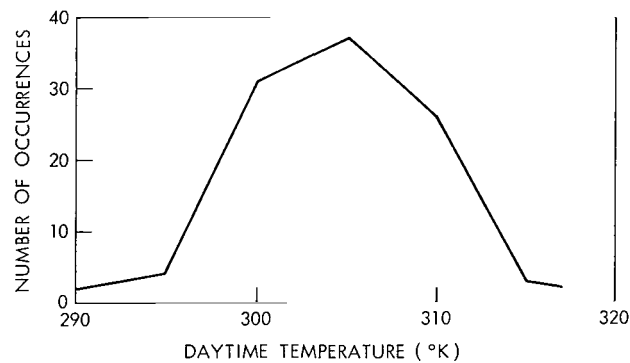

Figure 22—Frequency distribution of daytime temperature, HRIR II, May 22, 1966, Orbit 95, 34.5°N, 10.5°W.

Assumption of Additional Transmission Peaks of the Filters

The filters of both HRIR's have been very carefully measured by the manufacturer before they were mounted.* Besides this, filters of the same batch have been once more checked after the discrepancy became obvious. In no case was it possible to detect a secondary transmission of more than 0.01 percent. Thus it seems highly improbable that the error has been caused by additional transmission peaks.

Assumption of Filter Shift

In order to estimate the influence of a spectral filter shift, the relation between the relative error of reflectance and the wavelength shift has been calculated and plotted in Figure 24, assuming — for an easier calculation — a rectangular-shaped filter transmission curve. The reflectance value obtained by Nimbus I is more than 100 percent higher than that obtained by Nimbus II; a shift of more than 0.2μ would be needed to explain this. As Figure 24 shows further, this filter shift towards shorter wavelengths would at the same time cause nighttime temperatures about 10°K too low. Since this effect has never been observed, as the investigations of Allison and Kennedy have shown, a filter shift is also highly improbable. Moreover, so large a shift could hardly be explained. In principle, it could be caused by tilting the filter or by appropriate variations of its temperature. As investigations by Illsley (Reference 9) show, the tilting angle and the temperature deviation must be likewise improbably high. Thus an explanation of the error by a wavelength shift is also, from this standpoint, hardly possible, because we know that the variations of the housing temperatures of the radiometers are not higher than a few degrees, and great tilting angles cannot be explained in terms of the layout of the filter mounting.
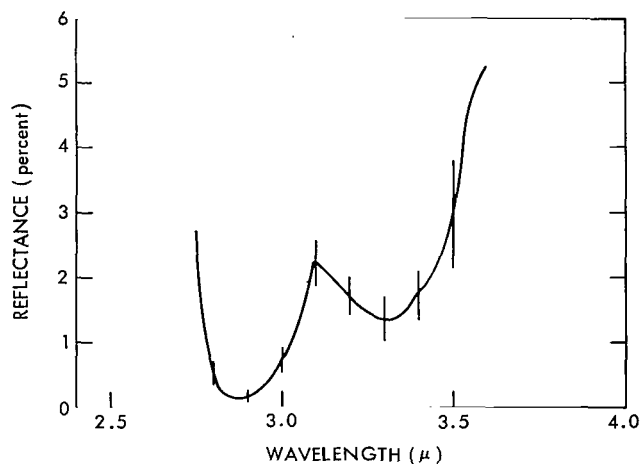

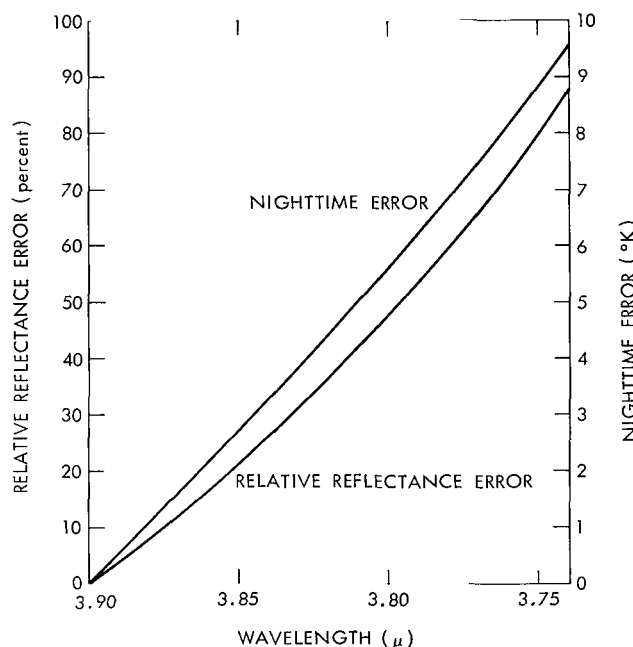Figure 23—Spectral cloud reflectance (after Reference 8).

Figure 24—Daytime and nighttime error vs peak transmission wavelength.

*Personal communication with the manufacturer of the interference filters.

Assumption of Additional Unfiltered Radiation

It seems unlikely that the error could be caused by direct sunlight entering the radiometer at the sun-oriented side through a defective housing, because the Nimbus satellite shields it from direct sun radiation. Moreover, the measured values should depend on the incidence angle of the sunlight—a relationship which actually did not exist, but the recorded intensity follows the nadir angle of the direction of the observation in a quite striking manner.

False light may also have reached the detector by passing through peeled-off parts of the filter. The percentage of the peeled-off filter area that is related to the radiance of 5×10^{-6} watts cm^{-2} $ster^{-1}$ has been calculated, assuming the following conditions:

1. Isotropic cloud reflectance between 1.5μ and 2.5μ of about 50 percent (after Hewson, Reference 4).

2. Total atmospheric water content of about 6 mm ppt water.

3. Short wavelength cut off by the Ge substrate of the filter at 1.5μ.

The windows between 1.5μ and 1.8μ and between 2.0μ and 2.5μ together contribute, under these assumptions, additional reflected radiation of 1.50×10^{-6} watts cm^{-2} $ster^{-1}$. The percentage of peeled-off filter area necessary is 0.3 percent. If filter size is considered, the value would be equivalent to an uncoated circular spot of 2.5 mm diameter, corresponding to an area of $5 mm^2$. It seems highly improbable that a peeling of this amount could have been caused by scratching. It seems more likely that this uncoated area comes from at least a part of the uncoated rim which every interference filter has because of the manufacturing process. This ring-shaped area, which generally shows a width of 1 or 2 mm, ought to be completely covered by the mounting. An estimate shows that a ring with a width of 0.05 mm uncovered by the filter mounting is sufficient to explain the discrepancy. Since both instruments have not been tested with short-wavelength radiation before launch, this explanation is highly probable.

Another question may arise: whether the filter has suffered a crack; for instance, during launch. In this case the faulty area can be even smaller because of the fact that now still more reflected sunlight, down to about 0.4μ, can be detected (albeit at a decreased responsivity of the detector). Again, taking into account the dimensions of the filter, a gap of only 0.03 mm is sufficient if the filter should have broken into two parts. It frequently occurs that filters subjected to shock break into just two parts; both parts stay in their positions, separated by a very small gap.

CONCLUSION

Three cases of observation of high-reflecting clouds have been investigated for each HRIR by means of frequency distributions. A mean value of cloud reflectance has been derived for each radiometer, and the intensity difference between the two has been determined.

Cloud reflectance measurements performed from an aircraft indicated that the HRIR of *Nimbus I was malfunctioning (resulting in too high effective temperatures)*. It certainly cannot be expected that the error can be located in a straightforward manner, because we have no access to the orbiting satellite. But it is possible to give more or less likely explanations, because of the excess of intensity recorded by Nimbus I. Thus the most probable cause seems to be an unlaminated filter area at the rim of the filter such as every interference filter shows and which in the case of Nimbus I was possibly not completely covered by the filter mounting, allowing the short-wavelength radiation to pass through the unlaminated filter area. Another assumption explains the excess intensity in terms of a cracked filter allowing short-wavelength radiation to penetrate the filter through the crack.

We will leave open the question as to whether the filter was improperly mounted or cracked or both. For future HRIR experiments, it seems advisable to perform a simple check of the spectral response of the instrument at short wavelengths. For example, it would be possible to vary the wavelength of radiation from a monochromatic source over the entire range of the solar spectrum while recording the radiometer output voltage. This procedure would allow the detection of even very small leaks and, further, provide a calibration in the short-wave part of the spectrum (if leaks were to exist), thus facilitating the interpretation of analyses such as those described above.

ACKNOWLEDGMENTS

REFERENCES

1. Catalog and User's Manual of Nimbus I and Nimbus II, NASA, Goddard Space Flight Center, 1965 and 1966.

2. "Observations from the Nimbus I Meteorological Satellite," NASA Special Publication No. 89, 1965.

3. Widger, W. K., Jr., Barnes, J. C., Merritt, E.S., and Smith, R. B., "Meteorological Interpretation of Nimbus High Resolution Infrared (HRIR) Data," final Report, Contract No. NAS 5-9554, Aracon Geophysics Co., Concord, Mass., August 1965.

4. Hewson, E. W., "The Reflection, Absorption and Transmission of Solar Radiation by Fog and Cloud," *Roy. Met. Soc. Quart. Journ.*, 69:47, 1943.

5. *World Atlas of Sea Surface Temperatures*, 2nd ed., published by the Hydrographic Office, United States Navy, 1944.

6. Allison, L. J., and Kennedy, J. S., "An Evaluation of Sea Surface Temperature as Measured by the Nimbus I High Resolution Infrared Radiometer," NASA Technical Note G-800, 1967.

7. Warnecke, G., Allison, L. J., and Foshee, L. L., "Observations of Sea Surface Temperatures and Ocean Currents from Nimbus II," GSFC Document X-622-67-435, 1967.

8. Blau, H. H., Jr., Duchane, E. M., et al., "Infrared Spectral Properties of High Altitude Clouds," prepared for Advanced Research Projects Agency, Contract No. NONR 3556 (00), 1963.

9. Illsley, R. F., "Preliminary Study of Low Temperature Effect on Interference Filters," Presentation at IRIS meeting, April 20, 1960.

"The aeronautical and space activities of the United States shall be
conducted so as to contribute . . . to the expansion of human knowl-
edge of phenomena in the atmosphere and space. The Administration
shall provide for the widest practicable and appropriate dissemination
of information concerning its activities and the results thereof."

— NATIONAL AERONAUTICS AND SPACE ACT OF 1958

NASA SCIENTIFIC AND TECHNICAL PUBLICATIONS

TECHNICAL REPORTS: Scientific and
technical information considered important,
complete, and a lasting contribution to existing
knowledge.

TECHNICAL NOTES: Information less broad
in scope but nevertheless of importance as a
contribution to existing knowledge.

TECHNICAL-MEMORANDUMS:
Information receiving limited distribution
because of preliminary data, security classifica-
tion, or other reasons.

CONTRACTOR REPORTS: Scientific and
technical information generated under a NASA
contract or grant and considered an important
contribution to existing knowledge.

TECHNICAL TRANSLATIONS: Information
published in a foreign language considered
to merit NASA distribution in English.

SPECIAL PUBLICATIONS: Information
derived from or of value to NASA activities.
Publications include conference proceedings,
monographs, data compilations, handbooks,
sourcebooks, and special bibliographies.

TECHNOLOGY UTILIZATION
PUBLICATIONS: Information on technology
used by NASA that may be of particular
interest in commercial and other non-aerospace
applications. Publications include Tech Briefs,
Technology Utilization Reports and Notes,
and Technology Surveys.

Details on the availability of these publications may be obtained from:

SCIENTIFIC AND TECHNICAL INFORMATION DIVISION

NATIONAL AERONAUTICS AND SPACE ADMINISTRATION
Washington, D.C. 20546